HemaSphere

EHA EUROPEAN HEMATOLOGY ASSOCIATION

Article
Open Access

Identifying Early Infections in the Setting of CRS With Routine and Exploratory Serum Proteomics and the HT10 Score Following CD19 CAR-T for Relapsed/Refractory B-NHL

Kai Rejeski[1,2,3,4], Viktoria Blumenberg[1,2,3,4], Gloria Iacoboni[5,6], Lucia Lopez-Corral[7,8], Soraya Kharboutli[4,9], Rafael Hernani[10], Agnese Petrera[11], Niklas Müller[1], Friederike Hildebrand[1], Lisa Frölich[1,3], Philipp Karschnia[12], Christian Schmidt[1], David M. Cordas dos Santos[1,3], José Luis Piñana[10], Fabian Müller[4,9], Ana Africa Martin[7,8], Martin Dreyling[1], Michael von Bergwelt-Baildon[1,3,4], Pere Barba[5,6], Marion Subklewe[1,2,3,4], Veit L. Bücklein[1,2,3,4]

GRAPHICAL ABSTRACT

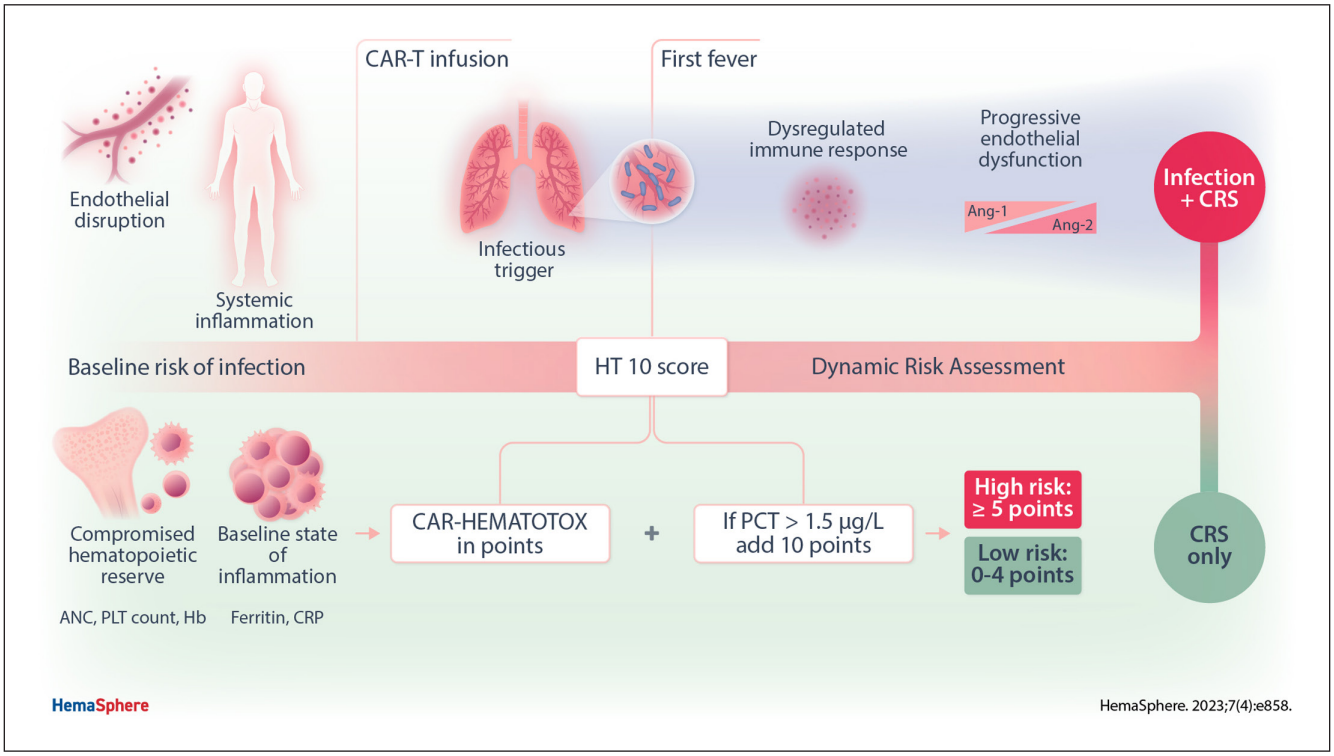

HemaSphere

EHA EUROPEAN HEMATOLOGY ASSOCIATION

Article
Open Access

Identifying Early Infections in the Setting of CRS With Routine and Exploratory Serum Proteomics and the HT10 Score Following CD19 CAR-T for Relapsed/Refractory B-NHL

Kai Rejeski[1,2,3,4], Viktoria Blumenberg[1,2,3,4], Gloria Iacoboni[5,6], Lucia Lopez-Corral[7,8], Soraya Kharboutli[4,9], Rafael Hernani[10], Agnese Petrera[11], Niklas Müller[1], Friederike Hildebrand[1], Lisa Frölich[1,3], Philipp Karschnia[12], Christian Schmidt[1], David M. Cordas dos Santos[1,3], José Luis Piñana[10], Fabian Müller[4,9], Ana Africa Martin[7,8], Martin Dreyling[1], Michael von Bergwelt-Baildon[1,3,4], Pere Barba[5,6], Marion Subklewe[1,2,3,4], Veit L. Bücklein[1,2,3,4]

Correspondence: Kai Rejeski (kai.rejeski@med.uni-muenchen.de).

ABSTRACT

Early fever after chimeric antigen receptor T-cell (CAR-T) therapy can reflect both an infection or cytokine release syndrome (CRS). Identifying early infections in the setting of CRS and neutropenia represents an unresolved clinical challenge. In this retrospective observational analysis, early fever events (day 0–30) were characterized as infection versus CRS in 62 patients treated with standard-of-care CD19.CAR-T for relapsed/refractory B-cell non-Hodgkin lymphoma. Routine serum inflammatory markers (C-reactive protein [CRP], interleukin-6 [IL-6], procalcitonin [PCT]) were recorded daily. Exploratory plasma proteomics were performed longitudinally in 52 patients using a multiplex proximity extension assay (Olink proteomics). Compared with the CRS^{only} cohort, we noted increased event-day IL-6 (median 2243 versus 64 pg/mL, $P = 0.03$) and particularly high PCT levels (median 1.6 versus 0.3 µg/L, $P < 0.0001$) in the patients that developed severe infections. For PCT, an optimal discriminatory threshold of 1.5 µg/L was established (area under the receiver operating characteristic curve [AUC_{ROC}] = 0.78). Next, we incorporated day-of-fever PCT levels with the patient-individual CAR-HEMATOTOX score. In a multicenter validation cohort (n = 125), we confirmed the discriminatory capacity of this so-called HT10 score for early infections at first fever (AUC_{ROC} = 0.87, $P < 0.0001$, sens. 86%, spec. 86%). Additionally, Olink proteomics revealed pronounced immune dysregulation and endothelial dysfunction in patients with severe infections as evidenced by an increased ANGPT2/1 ratio and an altered CD40/CD40L-axis. In conclusion, the high discriminatory capacity of the HT10 score for infections highlights the advantage of dynamic risk assessment and supports the incorporation of PCT into routine inflammatory panels. Candidate markers from Olink proteomics may further refine risk-stratification. If validated prospectively, the score will enable risk-adapted decisions on antibiotic use.

INTRODUCTION

Although chimeric antigen receptor T-cell (CAR-T) therapy has revolutionized the treatment landscape of relapsed/refractory (R/R) B-cell non-Hodgkin lymphoma (B-NHL),[1–8] it is accompanied by a unique toxicity profile that classically includes cytokine release syndrome (CRS) and immune effector cell associated neurotoxicity syndrome (ICANS).[9–11] Real-world evidence has further emphasized the importance of hematological toxicity as the most common high-grade toxicity of CAR-T therapy, which can present both as a syndrome of profound bone marrow aplasia,[12] or as prolonged cytopenia.[13–18] An additional expected on-target/off-tumor side effect of CD19-directed

[1]Department of Medicine III – Hematology/Oncology, University Hospital, LMU Munich, Germany
[2]Laboratory for Translational Cancer Immunology, LMU Gene Center, Munich, Germany
[3]German Cancer Consortium (DKTK), Munich Site, and German Cancer Research Center, Heidelberg, Germany
[4]Bavarian Cancer Research Center (BZKF), Partner Sites Munich and Erlangen, Germany
[5]Department of Hematology, Vall d'Hebron Institute of Oncology (VHIO), University Hospital Vall d'Hebron, Barcelona, Spain
[6]Department of Medicine, Universitat Autònoma of Barcelona (UAB), Bellaterra, Spain
[7]Hematology Department, Hospital Clínico Universitario de Salamanca, IBSAL, CIBERONC, Salamanca, Spain
[8]Centro de Investigación del Cáncer-IBMCC, Salamanca, Spain
[9]Department of Internal Medicine 5, Hematology and Oncology, Friedrich-Alexander-Universität Erlangen-Nürnberg and University Hospital Erlangen, Germany
[10]Hematology Department, Hospital Clínico Universitario, INCLIVA Research Institute, Valencia, Spain
[11]Metabolomics and Proteomics Core Facility, Helmholtz Zentrum Munich – German Research Center for Environmental Health, Munich, Germany
[12]Department of Neurosurgery, University Hospital, LMU Munich, Germany
Supplemental digital content is available for this article.

HemaSphere (2023) 7:4(e858).
http://dx.doi.org/10.1097/HS9.0000000000000858.
Received: August 23, 2022 / Accepted: February 6, 2023

CAR-T is B-cell aplasia and hypogammaglobulinemia.[19] The combination of cellular and humoral immunodeficiency translates into a predisposition for infectious complications, which substantially contribute to the toxicity burden and drive non-relapse mortality.[6,20–24] Infections, and particularly bacterial infections, usually occur during the first 30 days after CAR-T during a vulnerable phase in which coincident CRS can be observed.[21,23–25]

A more vexing and practical challenge encountered after CAR-T therapy lies in determining if an episode of early fever relates to infection versus CRS. The overwhelming majority of CAR-T patients develop CRS of any grade with pyrexia representing the cardinal symptom.[26] Due to the fact that most patients develop transient lymphodepletion-associated neutropenia,[13,27] cytokine storm typically presents as a syndrome of "febrile neutropenia." This usually triggers broad-spectrum antibiotic use—even in the absence of other clinical signs of infection or microbiologic evidence. For example, we recently demonstrated that a striking 86% of patients receive intravenous (IV) broad-spectrum antibiotics in the first 10 days after CAR-T infusion.[23] However, this comes at the price of antibiotic-specific side effects, the potential emergence of resistant strains, and selection for *Clostridium difficile* and *enterococci*.[28–32] Furthermore, antibiotics can negatively impact the intestinal micromilieu, which should be avoided considering the recently uncovered immunomodulatory role of the gut microbiome in the context of CAR-T specifically.[33–35] For these reasons, simple clinical tools that adequately discriminate between fever due to infection versus CRS are urgently needed. The clinical need for precise risk-stratification tools is especially pertinent as outpatient administration of CAR-T is being actively explored.[36]

We recently developed the CAR-HEMATOTOX (HT) score for CAR-T–related hematotoxicity.[13] The score is determined before lymphodepleting chemotherapy (day −5), incorporates factors of hematopoietic reserve (ANC, hemoglobin, platelet count) and inflammation (C-reactive protein [CRP], ferritin), and risk-stratifies patients into a high versus low risk for prolonged neutropenia. Importantly, the model also identifies patients at high risk for infectious complications and poor clinical outcomes.[23] Still, specificity was low and additional parameters may refine the predictive capacity of the score. Standard inflammatory marker panels that incorporate CRP, procalcitonin (PCT), and interleukin (IL)-6 represent an attractive option for dynamic risk assessment, as they are readily available and already implemented at most large CAR-T centers. While specific inflammatory signatures have been associated with severe CRS[37,38] and life-threatening infections[39,40] following CD19 CAR-T, these models often incorporate serum solutes that are not a part of the clinical routine or require long turn-around times (eg, IL-8, IL-1 beta, interferon-γ), limiting their broad use. Here, we therefore studied dynamic changes of routine serum inflammatory markers in the context of CD19 CAR-T, integrating information from baseline risk predictors. Furthermore, we explored longitudinal proteomic signatures emerging over time in patients that developed severe infections compared to CRS^{only} controls.

MATERIALS AND METHODS

Patient characteristics and clinical data collection

In this retrospective observational study, early infection events (day 0–30) and day-by-day CRS dynamics were characterized in 62 adult patients receiving standard-of-care axicabtagene ciloleucel (axi-cel, n = 23), tisagenlecleucel (tisa-cel, n = 30), or brexucabtagene autoleucel (brexu-cel, n = 9) for R/R B-NHL. Patients were treated between January 2019 and March 2022 (data cutoff) at the University Hospital of the LMU Munich, Germany. Participation in a clinical trial, or CAR-T treatment for a non–B-NHL disease entity represented key exclusion criteria. Lymphodepleting chemotherapy with fludarabine and cyclophosphamide was applied according to the manufacturers' instructions.[1,2] Clinical metadata and peripheral serum samples were collected with institutional review board approval (Project No. 19-817). The study was performed in accordance with the 1964 Helsinki declaration and its later amendments or comparable ethical standards. Informed written consent was obtained from all patients. Institutional guidelines for CRS, ICANS, and infection management are outlined in Suppl. Table S1.

Infection categorization and classification of severity

Infections were defined as bacterial, viral, or fungal on the basis of microbiologic/histopathologic data or as a clinical syndrome of infection (eg, pneumonia, cellulitis, cystitis) based on retrospective chart review. The study timeframe was 30 days from CAR-T infusion due to the expected maximum time window of coincident CRS.[41] All infections before infusion were excluded. Infection onset was specified as the day on which the diagnostic test was performed and/or the onset of symptoms. The clinical source of infection was determined from the combination of symptomology, microbiologic isolates, and radiographic findings. Fever alone, in the absence of clinical signs of infection or microbiologic data, was not counted as an infection. Infection severity was classified as mild, moderate, severe, life-threatening, or fatal according to previously established criteria.[21,42]

Index event categorization

CRS and ICANS were assessed prospectively according to ASTCT consensus criteria.[10] Cumulative incidence curves were calculated as time-to-event-analysis from Kaplan-Meier estimates for CRS 1°, CRS ≥2°, and severe infections; censoring the observation time on the date of progression, last follow-up, or death. We retrospectively defined fever events as infection versus CRS, with index events being categorized as the day on which the respective toxicity event occurred. For patients that developed CRS ≥2°, the first day with grade ≥2 CRS was defined as the event day.

Serum cytokine analyses

Serum inflammatory markers (CRP, PCT, IL-6) were measured daily from CAR-T infusion until discharge and on subsequent outpatient visits (weekly during the first month). Laboratory measurements were assessed at the Institute of Laboratory Medicine (University Hospital, LMU Munich). The temporal analyses of inflammatory markers over time were performed by computing the aggregate median value for each day between day 0 and 21. Differences between groups were explored using a mixed effects analysis considering both time and effect size using the restricted maximum likelihood method (GraphPad Prism v9.0).

Development of the HT10 risk classification system

The baseline HT and EASIX-FC scores were assessed before lymphodepletion (day −5) for all patients as previously described.[13,43] Inflammatory markers were tested using binary logistic regression for severe infections versus CRS index events. Discriminatory thresholds were determined from receiver operating characteristic (ROC) curves by optimizing the respective Youden *J* statistic. The "HT10" score was modeled for optimal discrimination of severe infections versus CRS control index events as determined by the highest area under the ROC curve (AUROC). Using the established PCT threshold, different values were added to the baseline HT score and the sum score was tested for discrimination. Metrics of score performance (eg, sensitivity, specificity) were assessed.

External validation of the HT10 score

Four European CAR-T centers participated in the confirmatory cohort of 125 r/r B-NHL patients receiving standard-of-care CD19 CAR-T. The 30-day cumulative incidence of viral and nonviral infections was assessed. The HT10 score was determined at time of first fever after CAR T-cell infusion. All patients received a standard diagnostic evaluation of underlying etiologies of fever as per institutional guidelines. Test characteristics were determined using ROC analysis studying if patients developed a severe infection during the first 30 days versus CRS only.

Longitudinal Olink plasma proteomic assays

The serum proteome was characterized across 4 sequential time points (days 0, 4, 14, 28) in 52 patients using a 92-protein multiplex proximity extension assay from the Olink platform ("Immuno Oncology Panel," Olink Bioscience). Experiments were performed as previously described.[44,45] Briefly, oligonucelotide-labeled monoclonal or polyclonal antibodies (PEA probes) were used to bind target proteins in a pairwise manner, thereby preventing all cross-reactive events. Upon binding, the oligonucleotides come in close proximity and hybridize, followed by extension, generating a unique sequence used for the digital identification of the specific protein assay.

A linear mixed model (LMM) was applied per protein that tested differences of serum proteins by patient group (infection versus CRS^{only} control) and time point. To account for potential confounding, age and sex were included as fixed effects, while a random effect per patient was included to account for potentially differing baselines. Regression models were fitted using the R-packages lme4 and lmerTest, while plots were generated using the OlinkAnalyze and ggplot2 packages. Protein levels were expressed in Normalized Protein eXpression (NPX) units, which were derived from Ct values. Because NPX is expressed in a log2 scale, a 1 NPX difference translates into a doubling of protein concentration.

Statistical considerations

Statistical significance was explored by nonparametric Mann-Whitney test for continuous variables and Fisher exact test for comparison of group variables. Correction for multiple testing was performed using the false discovery rate approach. Statistical analysis and data visualization was performed using GraphPad Prism (v9.0), SPSS (v26.0), or R Statistical Software (v4.1.2).

RESULTS

CRS and infection rates in a real-world cohort of CAR-T–treated B-NHL patients

Across all patients, the median age was 64 years (range 19–83), median ECOG was 1 (IQR 1–2), and the median international prognostic index (IPI) in evaluable LBCL patients was 2 (IQR 2–3) (Table 1). The study cohort focused on the patients that developed any-grade CRS or an infection (57 patients). Five patients

Table 1

Baseline Patient Demographic and Clinical Characteristics

	CRS 0°–1° (n = 35)[a]	CRS ≥2° (n = 27)	*P*	Other (n = 47)	Severe Infection (n = 15)	*P*
Age, years (95% CI)	61 (59-66)	65 (55-69)	0.65	64 (60-66)	60 (49-69)	0.65
Sex (female)	12 (34%)	12 (44%)	0.44	18 (38%)	6 (40%)	0.99
Prior autologous SCT	14 (40%)	6 (22%)	0.18	14 (30%)	6 (40%)	0.53
Median lines of prior therapy (excl. bridging. IQR)[b]	4 (3–5)	3 (2–4)	**0.04**	4 (2–4)	4 (3–4)	0.51
Median ECOG at lymphodepletion (IQR)[b]	1 (0–1)	1 (0–1)	0.70	0 (0–1)	1 (0.5–1)	0.09
IPI (IQR)[b]	2 (1–3)	2 (2–3)	0.99	2 (1.25–2.75)	3 (2–3.5)	**0.04**
Disease entity						
DLBCL, PMBCL	22 (63%)	13 (48%)	0.31	24 (51%)	11 (74%)	0.15
Transformed lymphoma	8 (23%)	10 (37%)	0.27	16 (34%)	2 (13%)	0.19
Mantle cell lymphoma	5 (14%)	4 (15%)	0.99	7 (15%)	2 (13%)	0.99
CAR product						
4-1BB (Tisa-cel)	17 (49%)	13 (48%)	0.99	24 (51%)	7 (47%)	0.99
CD28z (Axi-cel, KTX-19)	18 (51%)	14 (52%)		23 (49%)	8 (53%)	
Tumor burden						
LDH (U/L), 95% CI	239 (174-319)	229 (201-381)	0.46	230 (199-290)	237 (143-390)	0.91
STLV (mm^3, IQR)[b]	60 (7–218)	130 (33–488)	0.08	61 (15–260)	205 (45–442)	0.12
Risk Classification Systems						
CAR-HEMATOTOX Score (Rejeski et al[13]), IQR	3 (1–4)	1 (0–3)	0.10	2 (1–3)	5 (2–6)	**0.002**
EASIX-F Score (Greenbaum et al[43]), IQR	1 (0–1)	1 (0–2)	0.90	1 (0–1)	1 (1–2)	**0.04**
Laboratory characteristics						
C-reactive protein (mg/dL), 95% CI	1.4 (0.8-3.1)	0.9 (0.2-3.6)	0.43	0.8 (0.3-1.4)	3.1 (1.3-4.5)	**0.01**
Ferritin (ng/mL), 95% CI	830 (348-1450)	496 (180-1272)	0.48	456 (284-830)	1978 (1062-2878)	**0.001**
Abs. lymphocyte count (G/L), 95% CI	460 (378-736)	550 (421-752)	0.59	550 (430-740)	411 (212-720)	0.20
Abs. neutrophil count (G/L), 95% CI	1690 (950-2260)	2380 (1830-3510)	**0.03**	1970 (1770-2590)	1350 (580-2330)	**0.05**
Platelet count (G/L), 95% CI	139 (104-175)	126 (76-230)	0.87	146 (116-185)	70 (20-178)	**0.05**
Hemoglobin (g/dL), 95% CI	9.0 (8.5-10.1)	9.8 (9.4-10.5)	0.13	10.0 (9.6-10.3)	8.6 (7.6-9.0)	**0.003**

[a]Five patients did not develop CRS of any grade, these patients did not develop an infectious complication.

[b]LBCL only.

All *P* values <0.05 are highlighted in bold.

CAR = chimeric antigen receptor; CI = confidence interval; CRS = cytokine release syndrome; DLBCL = diffuse large B-cell lymphoma; ECOG = Eastern Cooperative Oncology Group; IPI = International Prognostic Index; IQR = interquartile range; LBCL = large B-cell lymphoma; LDH = Lactate Dehydrogenase; PMBCL = primary mediastinal B-cell lymphoma; SCT = stem cell transplantation; STLV = sum of target lesion volume.

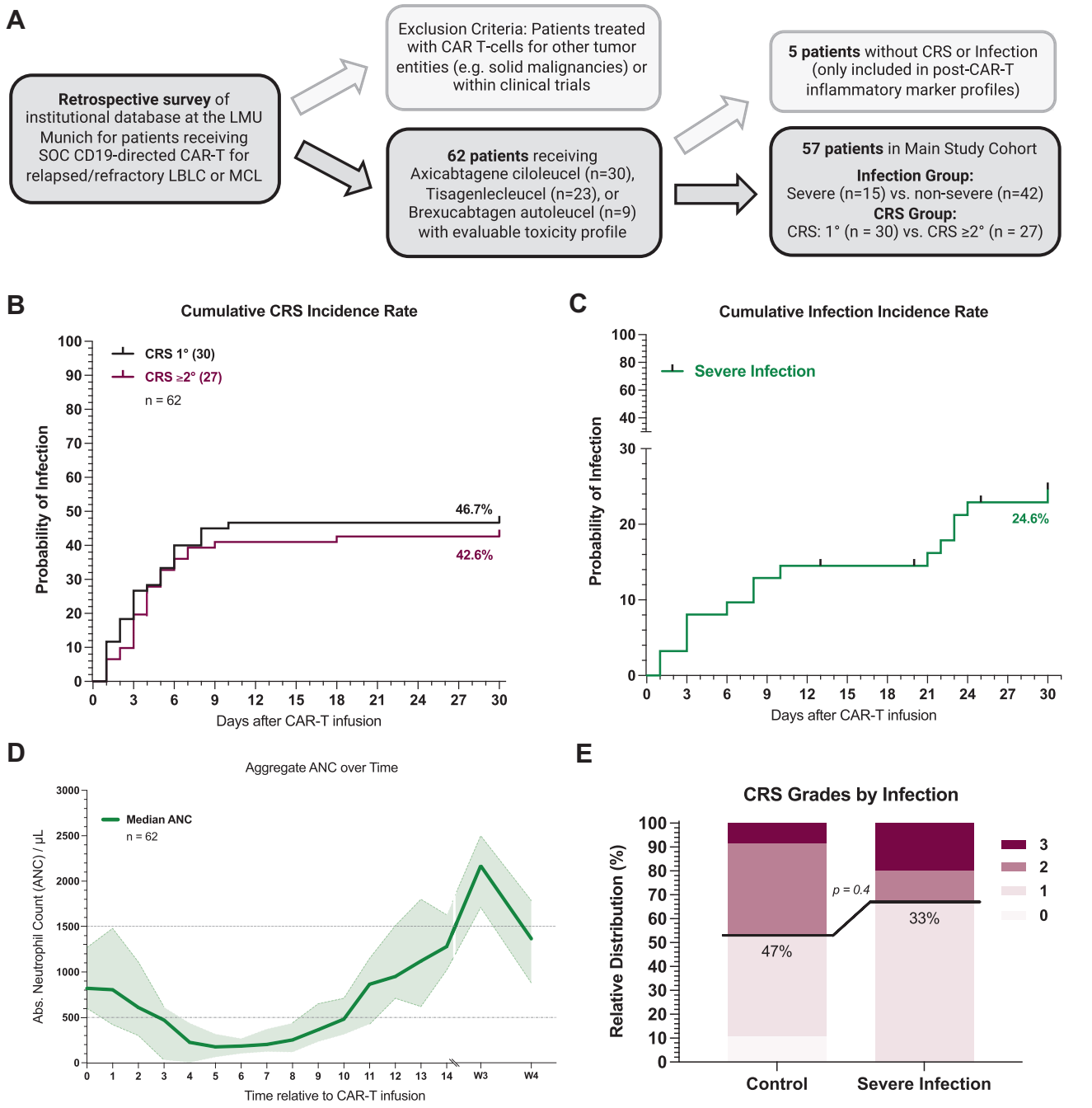

Figure 1. CRS and infection rates in a real-world cohort of CAR-T–treated B-NHL patients. (A) Schematic overview of the study cohort with key inclusion and exclusion criteria. (B) Cumulative incidence rate of CRS grade 1 (gray) and CRS grade ≥2 (magenta) in the first 30 d after CAR-T infusion. (C) Cumulative incidence rate of severe infection (green) in the first 30 d after CAR-T infusion. Severe infections were defined as requiring i.v. anti-infective therapy and/or hospitalization and microbiologic evidence of infection. In the absence of microbiologic evidence overwhelming evidence of clinical infection had to present (eg, clinical symptoms and concordant imaging findings. (D) Aggregated median ANC over time for 62 patients between day 0 (CAR infusion) and day 30. Light shading depicts the 95% CIs of the median for each time point. (E) Relative distribution of CRS grades according to ASTCT grading in patients with severe infection (n = 15) and without severe infection events (n = 47). B-NHL = B-cell non-Hodgkin lymphoma; CAR-T = chimeric antigen receptor T-cell therapy; CI = confidence interval; CRS = cytokine release syndrome.

developed neither CRS nor an infection and were excluded from subsequent analyses (Figure 1A). Demographic and laboratory characteristics were balanced between the patients with mild CRS (ASTCT 1°) versus moderate-to-severe CRS (ASTCT ≥2°). No significant difference in baseline EASIX-FC scores was observed. On the other hand, patients that developed a severe infection had a higher median ECOG (2 versus 1, $P = 0.01$) and IPI (3 versus 2, $P = 0.07$) at baseline compared with the CRS^{only} control. Notably, at baseline, the infection group exhibited high levels of systemic inflammation (median ferritin 1978 versus 456 ng/mL, $P = 0.002$) and impaired hematopoietic reserve (median hemoglobin 8.6 versus 10.0 g/dL, $P = 0.003$), which was further reflected by higher HT scores (median 5 versus 2, $P = 0.002$).

The cumulative 30-day incidence of grade 1° and grade ≥2° CRS was 47% and 43%, respectively (Figure 1B). Patients with grade ≥2° CRS displayed earlier CRS onset (median 1 versus 3 days) and longer CRS duration (median 8 versus 4 days) compared with their mild CRS counterparts (Suppl. Table S2). Most patients with grade

≥2° CRS exhibited previous grade 1° CRS (19/27, 70%), lasting a median of 2 days (IQR 1–2). The anti–IL-6 receptor antagonist tocilizumab was applied in the overwhelming majority of CRS patients, irrespective of CRS severity (1°: 90%, ≥2°: 100%), reflecting the institutional practice of tocilizumab application in case of fever >24 hours. Still, grade ≥2° CRS patients more frequently received high-dose glucocorticosteroids and developed more severe ICANS (Suppl. Table S2), consistent with prior reports.[23]

A total of 15 patients developed a severe infectious complication for a cumulative 30-day incidence of 24.6% (Figure 1C). This included 9 bacterial infections, 2 fungal infections, and 4 patients with a clinical syndrome of infection (2 central line infections, 2 pneumonias). Median infection onset was on day 8 (IQR 3–23), commonly occurring in the setting of coincident severe neutropenia (ANC <500/µL) (Figure 1D). Indeed, neutropenia was observed in 37 of 57 (65%) CRS events and 9 of 15 (60%) infection events. Grade 2 or higher CRS was noted in 33% of the patients with a severe infection compared with 47% of the patients without (Figure 1E). We did not find a significant correlation between CRS grade and severe infections ($G^2 = 0.13$, P = n.s., Suppl. Figure S2). Notably, severe infections were associated with a prolonged duration of neutropenia (median 13 versus 8.5 days, $P = 0.01$) and a higher frequency of an aplastic phenotype of neutrophil recovery[13] (47% versus 9.5%, $P = 0.004$) (Suppl. Table S2 and Suppl. Figure S1). Furthermore, patients that developed severe infections displayed a prolonged duration of high-dose glucocorticosteroid use, and more frequently required an intensive care unit admission.

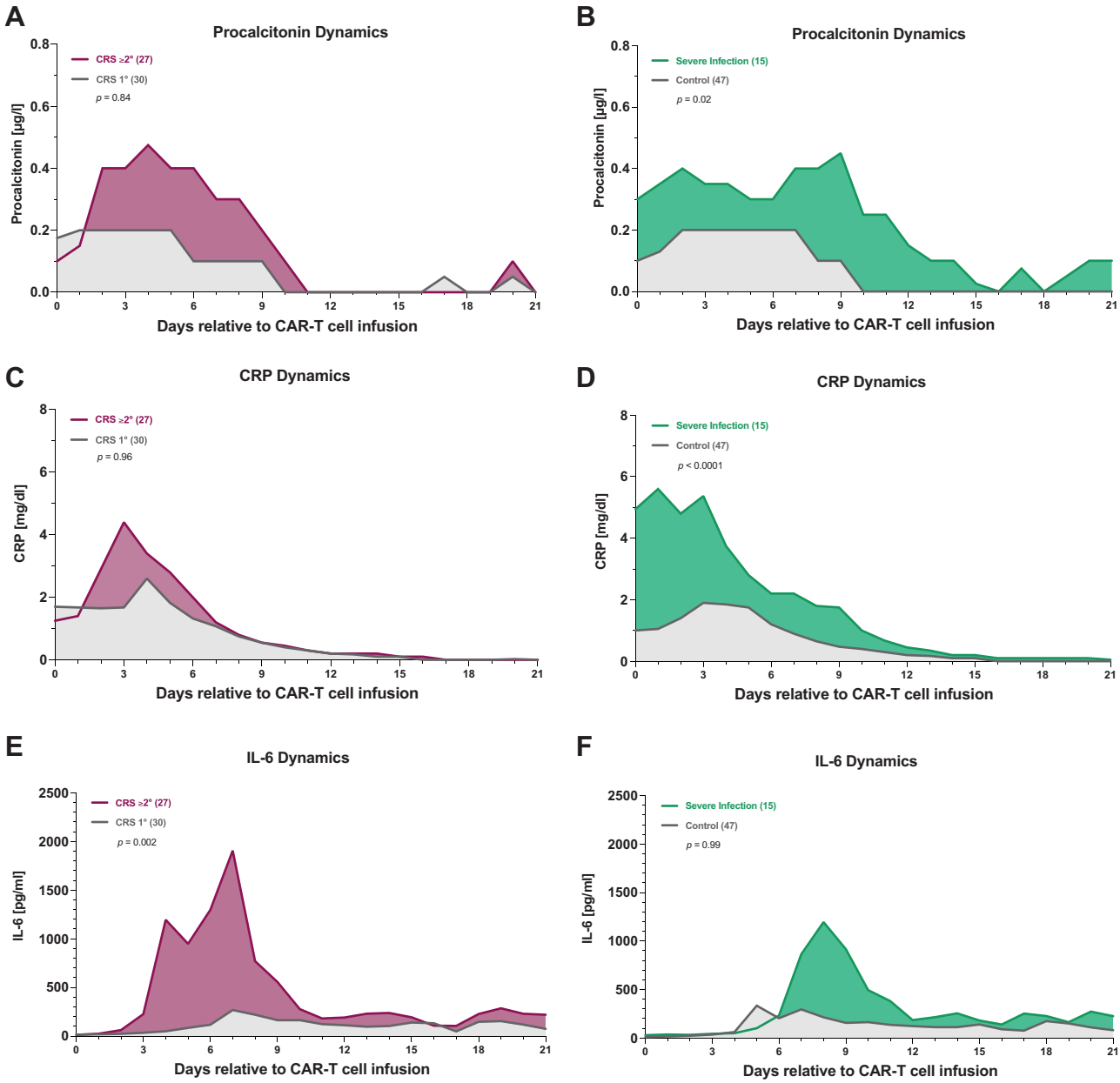

Figure 2. High-grade CRS is characterized by high interleukin-6 levels, while severe infections are marked by baseline inflammation high procalcitonin levels. (A–B) Aggregated median procalcitonin values over time during the first 21 d after CAR-T infusion by CRS grade (A) and presence of severe infection (B). (C–D) Aggregated median CRP values by CRS grade (C) and presence of severe infection (D). (E–F) Aggregated median interleukin-6 values by CRS grade (E) and the presence of severe infection (F). Serum samples were prospectively collected in a laboratory panel that was performed at least daily during the first 2 wk and then as indicated. Significance values were determined with a mixed effects analysis considering both time and effect size. CAR-T = chimeric antigen receptor T-cell therapy; CRS = cytokine release syndrome.

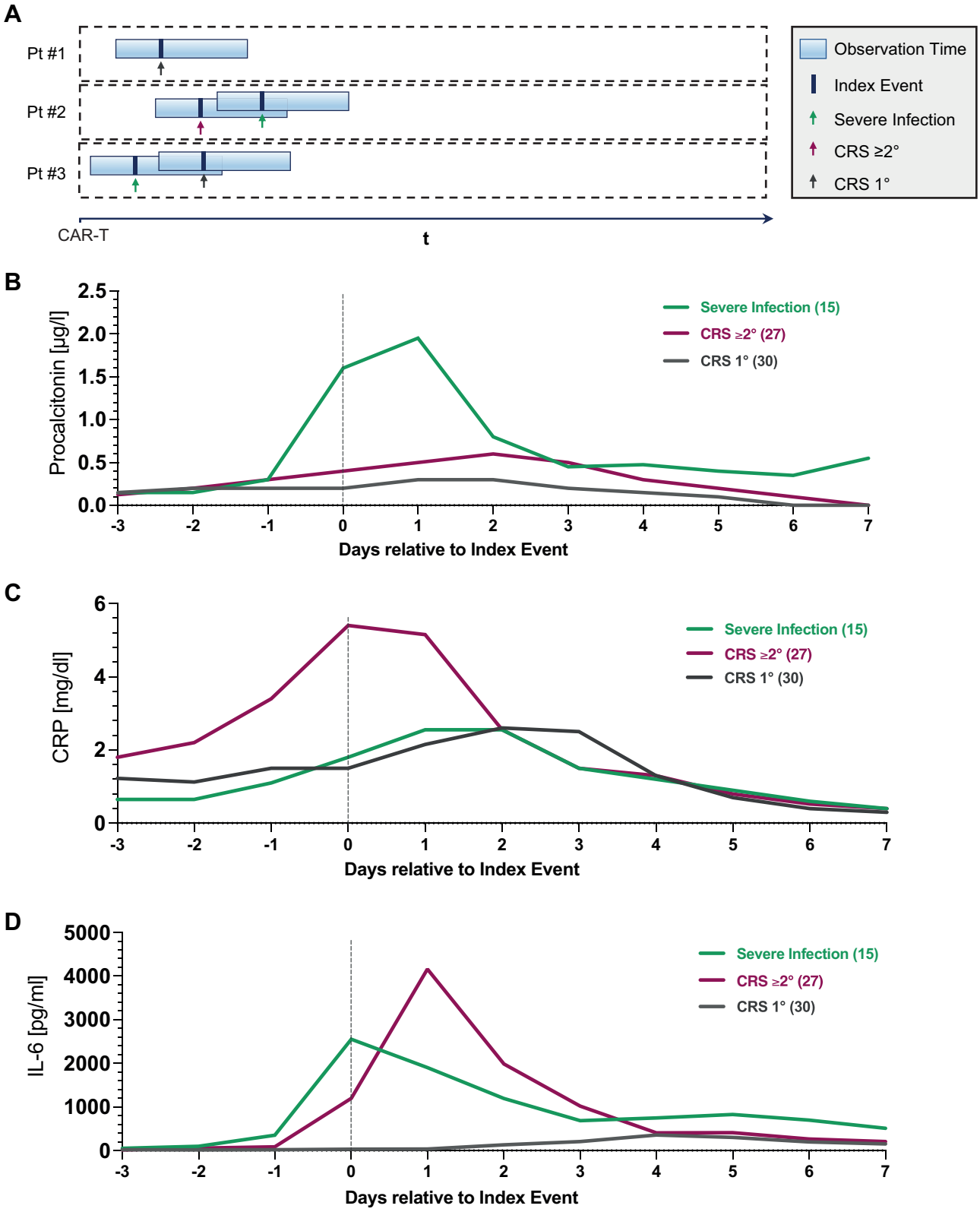

Figure 3. Serum inflammatory dynamics by index event. (A) Graphical representation of index event analysis: hypothetical patient #1 displays early grade 1 CRS and no infections; patient #2 displays grade early 2 CRS followed by a severe infection; patient #3 displays an early severe infection followed by grade 1 CRS. Serum procalcitonin (B), CRP (C), and IL-6 (D) levels were retrospectively assessed relative to the respective index event (severe infection: green; grade 1 CRS: gray; grade ≥2 CRS: magenta). The aggregated median values are depicted. CRP = C-reactive protein; CRS = cytokine release syndrome; IL-6 = interleukin-6.

High-grade CRS is characterized by high interleukin-6 levels, while severe infections are marked by baseline inflammation and high PCT levels

Next, we studied dynamic changes in serum inflammatory marker profiles over time in patients with CRS grade 1° versus ≥2°, and in CRS patients with and without a severe infection. Following CD19 CAR-T infusion, patients with grade ≥2° CRS displayed significantly elevated day 0–21 levels of IL-6 compared with their grade 1° CRS counterparts (P = 0.002, Figure 2E). On the other hand, CRP and PCT levels were not significantly altered in a mixed effects analysis accounting for both time and marker elevation (Figure 2A, C). In patients with infectious complications, PCT levels were significantly increased over time (P = 0.02, Figure 2B). Furthermore, CRP levels were significantly increased (P < 0.0001, Figure 2D), though this was particularly evident close to CAR-T infusion (day 0–3), further underlying the higher risk of infection in patients with baseline inflammation (Table 1). The mixed effects model did not detect significant changes in IL-6 levels over time between patients with and without infection (Figure 2F).

To elucidate distinct inflammatory signatures in relation to a specific toxicity event (CRS 1° versus CRS ≥2° versus severe infection), we performed "index event analyses" that take a retrospective snapshot of laboratory constellations on a day of interest (Figure 3A, Table 2). While all inflammatory markers were significantly increased on the index-event day in patients with grade ≥2° versus 1° CRS, this was especially noted for CRP (median 5.4 versus 1.5 mg/dL, P = 0.001, Figure 3C) and IL-6 (median 1196 versus 30.7 pg/mL, P < 0.001, Figure 3D), though this was likely influenced by prior tocilizumab exposure for previous grade 1° CRS. On the other hand, the severe infection index events were characterized by particularly high PCT levels (median 1.6 versus 0.3 µg/L, P = 0.001, Figure 3B) compared with the respective CRS controls. Of interest, we did not find significant differences in neutrophil counts by index event group, suggesting that both CRS and infection typically occur during a phase of coincident neutropenia (Figure 1D).

ROC analyses were performed to study how the inflammatory markers discriminate for the respective endpoints of grade ≥2° versus grade 1° CRS (= CRS index event), as well as severe infection versus any-CRS control (= infection index event) (Table 3). For the CRS index event, the highest AUC was observed for IL-6 (AUC_{ROC} = 0.95, P < 0.001) with an optimal discriminatory threshold of 77 pg/mL. The sensitivity and specificity were 89% and 93% at this threshold, respectively. Conversely, the highest discrimination between severe infectious complications and CRS was observed for serum PCT (AUC_{ROC} = 0.78, P = 0.0007, Figure 4A). An optimal discriminatory threshold was established at a PCT level of 1.5 µg/L (sensitivity = 60%, specificity = 91%).

Combining the baseline CAR-HEMATOTOX with index-event serum PCT increases the discriminatory capacity for severe infections in the setting of CRS

Although the baseline HT score was associated with severe infections (AUC_{ROC} = 0.75, P = 0.003, Figure 4B), the observed specificity was low at 47%. On the basis of the above findings, we tested if serum PCT values improve upon the baseline prognostication of infection risk with the HT score (Table 1). Differently weighted combinations of the score and the established PCT threshold (1.5 µg/L) were analyzed in regards to their capacity to identify severe infections (Suppl. Table S3). Optimal test characteristics were observed with the addition of 10 points to the patient-specific HT score in case of serum PCT levels ≥1.5 µg/L on the event day. This so-called "HT10" score displayed superior discrimination for severe infections on ROC analysis (AUC_{ROC} 0.92, P < 0.0001, sensitivity 80%, specificity 91%, Figure 4C) when compared with the HT score or PCT alone (Figure 4A-B, Suppl. Figure S3). Furthermore, the "HT10" score was strongly associated with severe infections on binary logistic regression analysis (G^2 = 34.13, P < 0.0001, Figure 4D). We found that the risk of an infection versus only CRS was highest in

Table 2

Serum Inflammatory Markers on the Index Event Day

	CRS Index Event			Infection Index Event		
Lab Parameter	**CRS 1° (n = 30)**	**CRS ≥2° (n = 27)**	***P***	**CRS Control (n = 57)**	**Severe Infection (n = 15)**	***P***
Procalcitonin (µg/L, 95% CI)	0.2 (0.2-0.3)	0.4 (0.2-0.7)	0.002	0.3 (0.2-0.4)	1.6 (0.3-5.8)	0.001
Median CRP (mg/dL, 95% CI)	1.5 (1.1-3.7)	5.4 (3.3-7.5)	0.001	3.45 (1.8-5.4)	1.8 (1.3-5.5)	0.37
Median IL-6 (pg/mL, 95% CI)	30.7 (18.4-42.7)	1196 (200-3525)	<0.001	63.8 (36.4-137)	2423 (44-13481)	0.04
ANC (G/L)	510 (0-1290)	340 (0-1270)	0.21	340 (95-1115)	680 (0-1860)	0.56

Laboratory parameter on the day of the index event. *P* values were determined by Mann-Whitney test. Correction for multiple testing was performed using the false discovery rate approach (2-stage step-up method of Benjamini, Krieger and Yekutieli).

ANC = absolute neutrophil count; CI = confidence interval; CRP = C-reactive protein; CRS = cytokine release syndrome; IL-6 = interleukin-6.

Table 3

Receiver Operating Characteristic Analyses

Laboratory Parameter	Discriminatory Threshold	AUC	*P* Value AUC	Sens.	Spec.
CRS index event					
Procalcitonin	0.4 µg/L	0.70	0.007	66%	80.0%
CRP	1.83 mg/dL	0.73	0.003	89%	60%
IL-6	77 pg/mL	0.95	<0.001	89%	93%
Infection index event					
CRP	N/A	0.58	0.37	N/A	N/A
IL-6	1553 pg/mL	0.68	0.03	60%	81%
Procalcitonin	1.5 µg/L	0.78	<0.001	60%	91%

ROC analyses were computed for the predicted probability of severe infection (infection index event) vs any-CRS control and CRS ≥2° vs CRS 1° (CRS index event). Serum inflammatory markers are sorted from top to bottom in the order of optimal discrimination determined by AUC for the respective index event. Discriminatory thresholds were determined based on ROC analyses computed for the predicted probability of grade ≥2 CRS vs grade 1 CRS (CRS index event), as well as the probability of severe infection vs CRS^{only} control (infection index event).

CRP = C-reactive protein; CRS = cytokine release syndrome; IL-6 = interleukin-6; ROC = receiver operating characteristic.

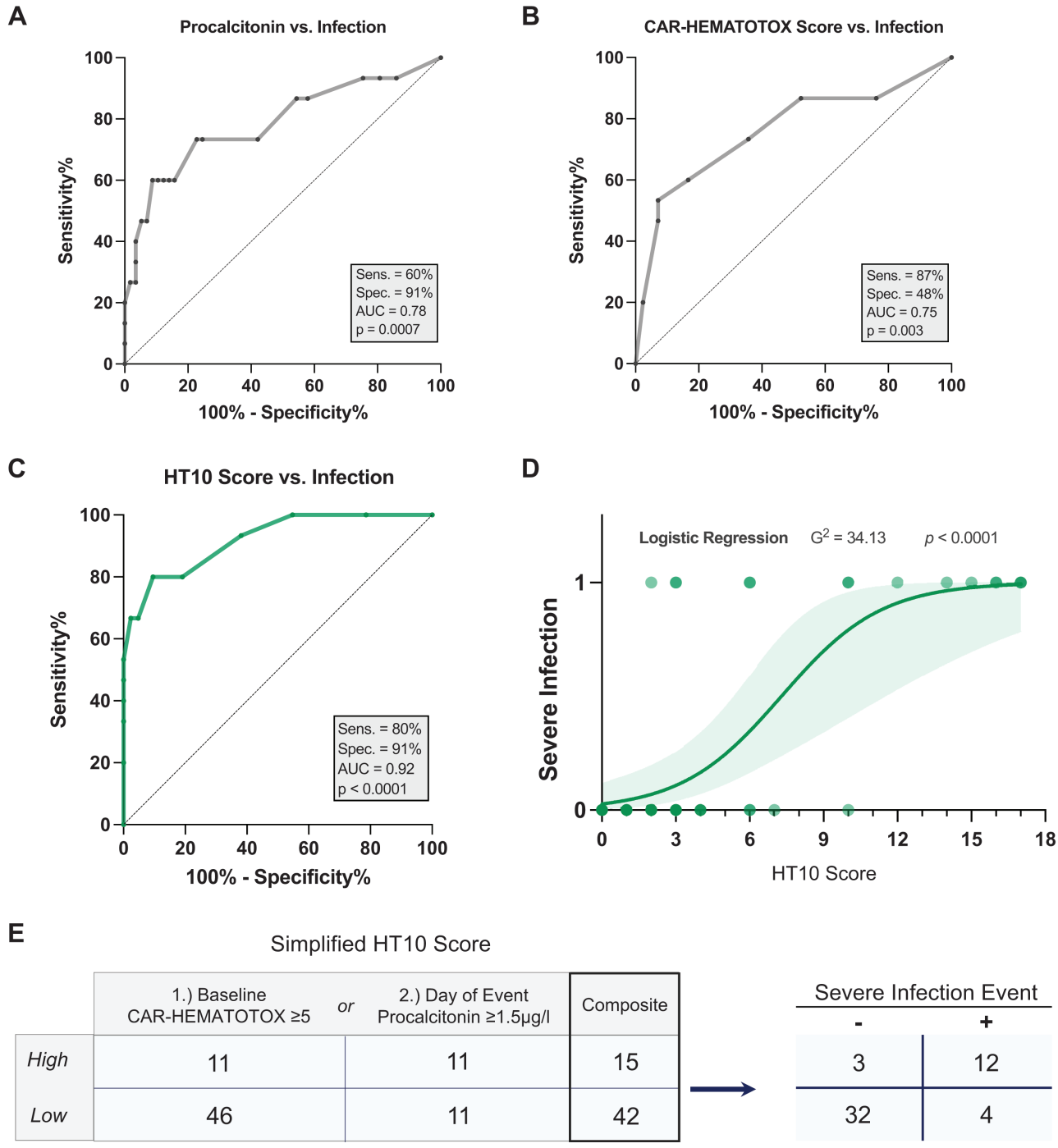

Figure 4. Combining the baseline CAR-HEMATOTOX with index-event serum procalcitonin increases the discriminatory capacity for severe infection events. Results of the receiver operating characteristic analyses comparing procalcitonin alone (A) or CAR-HEMATOTOX score alone (B) against the binary outcome of severe vs nonsevere infection. (C) ROC analysis studying the influence of a combined CAR-HEMATOTOX and procalcitonin ("HT + PCT10") score on the binary outcome of severe vs nonsevere infection. In the case of a PCT level ≥1.5 µg/L, an additional 10 points were added to the baseline CAR-HEMATOTOX score. The respective area under the curve and *P* value of the ROC curve are depicted. (D) Binary logistic regression analysis comparing the association between the "HT + PCT10" score and the binary outcome of severe vs nonsevere infection. The *P* value is shown for the likelihood ratio test (G^2); light shading indicates the 95% asymptotic confidence bands. (E) Simplified HT10 Score: The composite number of patients fulfilling the criteria for a high score (either baseline CAR-HEMATOTOX score ≥5 or day-of-event PCT ≥1.5 µg/L) and the relation to the endpoint of severe infection is depicted. CAR = chimeric antigen receptor; PCT = procalcitonin; ROC = receiver operating characteristic.

case of a baseline HT score ≥5 and/or an event-day PCT greater than 1.5 µg/L (simplified HT10 score, Figure 4E). These data highlight that the combination of both patient-level baseline risk (HT score), and dynamic changes in select serum inflammatory markers such as PCT, can help to identify severe infections in the setting of CRS.

The HT10 score discriminates for early infections at first fever in an external validation cohort

To test the external validity of the "HT10" score, we studied early infections and CRS in a confirmation cohort of 125 patients treated with CD19 CAR-T for r/r B-NHL across 4 CAR-T sites (Vall d'Hebron Barcelona, Erlangen, Valencia, Salamanca). A

total of 144 patients were screened: 8 non–B-NHL patients and 11 patients without available PCT measurements were excluded from the analysis (Suppl. Figure S4). Relevant baseline patient features and toxicity results are provided in Suppl. Table S4. Patients in the confirmation cohort exhibited fewer lines of prior therapy, had lower hemoglobin and ECOG performance status, but also displayed higher median LDH and IPI at lymphodepletion. The rate of severe infections during the first 30 days was 21%; the rate of severe CRS was 10%, both comparable to the training cohort (Suppl. Table S5). Toxicity management was similar between both cohorts with tocilizumab being applied in 78% of cases. Of interest, 68% of the patients in the confirmation cohort received an antibiotic prophylaxis with a fluoroquinolone. On ROC analysis, the HT10 score reliably identified patients at time of first fever after CAR T-cell infusion that went on to develop a severe infection as opposed to only CRS (AUC 0.87, $P < 0.001$, sensitivity 86%, specificity 86%, Figure 5A). In HT10^{high} patients (eg, score ≥5), we observed an increased rate of all-grade infections (58% versus 21%, $P < 0.001$) and especially severe infections (58% versus 8%, $P < 0.001$) (Figure 5B). The difference in infection rates were more pronounced when specifically analyzing nonviral infections (severe infections: 55% vs 3%, $P < 0.0001$; Figure 5C). Accordingly, the cumulative 30-day incidence of severe infections was increased in the HT10^{high} patients (Figure 5D), particularly for nonviral infections (Figure 5E). The first nonviral infection was noted on day +19 in the HT10^{low} group, with a 30-day incidence of only 3.3%. Overall, we found that the majority of infections occurred within the first 20 days in the confirmation cohort.

Longitudinal proteomic analysis reveals that patients with severe infections display progressive endothelial dysfunction and severe immune dysregulation

Inflammatory marker patterns were further characterized in 13 severe infection patients (all with coincident CRS) compared with 39 CRS^{only} controls. A total of 201 samples were studied across 4 time points resulting in 21.068 unique data points. Principal component analysis of the NPX distribution did not identify any potential outliers, and only a single sample was flagged with a quality control warning (Suppl. Figure S5). To identify proteins differential between infection versus CRS^{only} conditions, LMM were fitted to each patient accounting for both infection status and time effects and adjusting for age, sex, and patient baseline.

Prior to CAR infusion (day 0), we found that the patients that subsequently developed infections already displayed significant protein-level changes compared with their CRS^{only} counterparts (top left, Figure 6A). For several proteins, such as *TNFRSF12A* and *CXC3L1,* these protein-level differences were conserved across multiple time points (Figure 6A). A total of 16 candidate

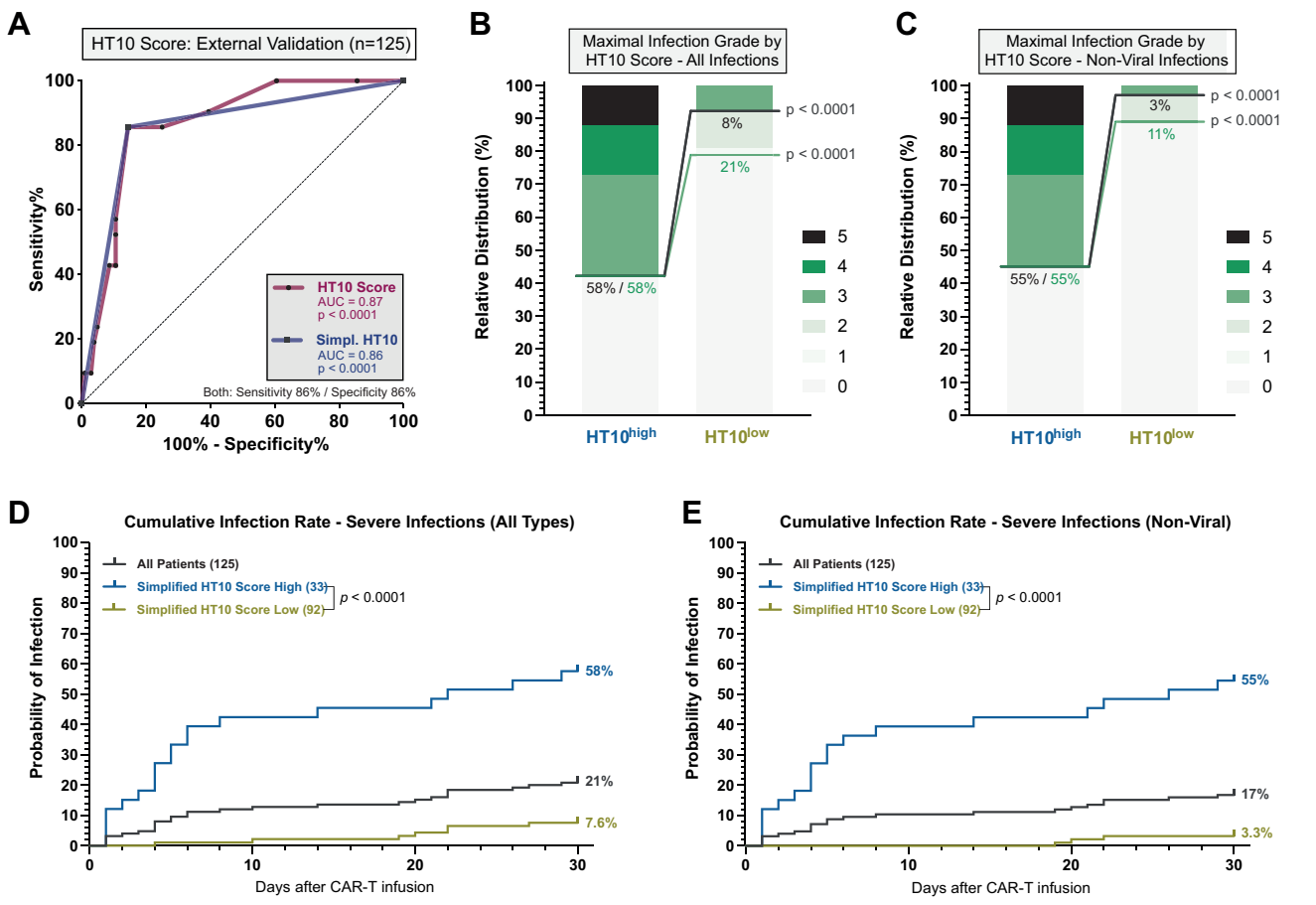

Figure 5. External validation of the discriminatory capacity of the HT10 score at time of first fever. (A) ROC analysis studying the influence of the HT10 score (magenta) and simplified HT10 score (blue), determined at time of first fever on the binary outcome of severe infection vs CRS only during the first 30 d after CAR T-cell infusion. The respective area under the curve, *P* value of the ROC curve, and sensitivity/specificity are depicted. (B–C) Relative distribution of infection grades for all infection subtypes (B) and nonviral infections only (C) during the first 30 d comparing HT10 high vs low patients. Infection grades (1°–5°) are color-coded in shades of green with the connecting green and gray lines and percentage numbers comparing all-grade and grade ≥3 infections, respectively, in HT10 high vs low patients. Significance values were determined by Fisher exact test (*$P < 0.05$, **$P < 0.01$, ***$P < 0.001$, ****$P < 0.0001$). (D) Cumulative 30-d incidence on all infection types (viral, bacterial, fungal, clinical syndromes of infection) by HT10 score. (E) Cumulative 30-d incidence of only nonviral infections HT10 score. CAR = chimeric antigen receptor; CRS = cytokine release syndrome; ROC = receiver operating characteristic.

proteins significantly differed by patient group. These top candidate proteins were heavily involved in biological processes related to inflammation, immune response, angiogenesis, and endothelial function (Suppl. Table S6–7). Hierarchical clustering of patients using the differentially expressed candidate proteins demonstrated a clear separation of the majority of severe infection from CRS^{only} patients (Figure 6B). Upregulated proteins in the severe infection group included *TNFRSF12A, CXC3L1, CCL20, CXCL13*, and *IL-15* (Figure 6C). On the other hand, soluble *CD40-L, ANGPT1,* and *EGF* were downregulated. Of interest, we observed upregulation of *ANGPT2* over time (adjusted $P = 0.019$, Figure 7A) while *ANGPT1* was downregulated (adjusted $P = 0.027$, Figure 7A)—indicating an increased angiopoietin-2 to angiopoietin-1 ratio in the patients that developed severe infections. Endothelial dysfunction was further reflected by downregulation of *FGF2* (adjusted $P = 0.026$, Figure 7A) and marked upregulation of *TNFRSF12A* (adjusted $P = 4.8E-05$, Figure 7A). In terms of proteins related to inflammatory response, we detected dysregulation of the CD40/CD40L axis with upregulation of *CD40* (adjusted $P = 0.049$, Figure 7B) and downregulation of *CD40L* (adjusted $P = 0.029$, Figure 7B) in the severe infection group. Furthermore, the innate immune regulators *CXC3L1, CCL20,* and *CXCL13* were elevated. Taken together, these longitudinal proteomic studies highlight progressive immune dysregulation and endothelial dysfunction in CAR T-cell patients developing infectious complications as opposed to only CRS.

DISCUSSION

In this retrospective observational study of 62 patients treated with CD19 CAR-T for B-NHL, we found that severe infections typically present with increased index-day PCT levels. Combining the baseline HT score with day-of-event PCT levels enhanced

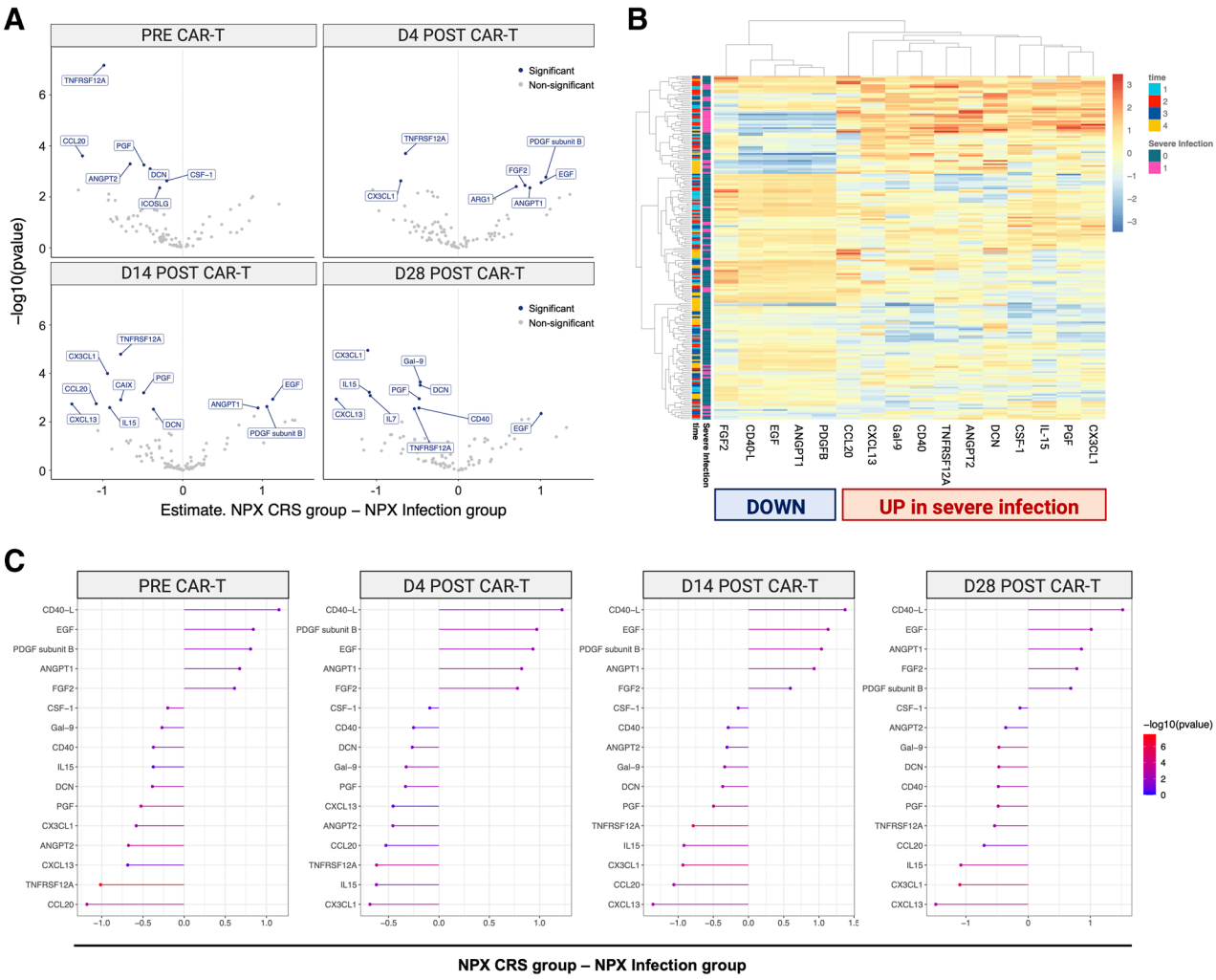

Figure 6. Severe infections are associated with distinct inflammatory signatures compared with CRS only controls. (A) Volcano plots showing the estimated mean difference between infection and CRS^{only} patients (x-axis), and corresponding –log10 (*P* values) (y-axis). Colors indicate proteins that passed the multiple testing adjusted *P* value threshold of $P < 0.05$. Each panel corresponds to one timepoint (days 0, 4, 14, 28). (B) Heatmap depicting normalized and centered NPX values (color scale) of the 16 proteins that differed between infection and CRS^{only} patients (significant main and/or interaction effect). Each row corresponds to a sample, and each column to a protein. Both rows and columns are sorted by hierarchical clustering, with dendrograms showing the clustering result. Time and severe infection status are indicated by the leftmost columns. (C) Differential expression per timepoint (from left to right) of the 16 proteins that differed between infection and CRS^{only} patients (significant main and/or interaction effect). The x-axis depicts the estimated mean difference between infection and CRS^{only} patients, and colors indicate the corresponding *P* values (not corrected for multiple testing). Each panel corresponds to one timepoint, with proteins sorted by NPX level changes (right: downregulated; left: upregulated in the Infection group). CRS = cytokine release syndrome; NPX = Normalized Protein eXpression.

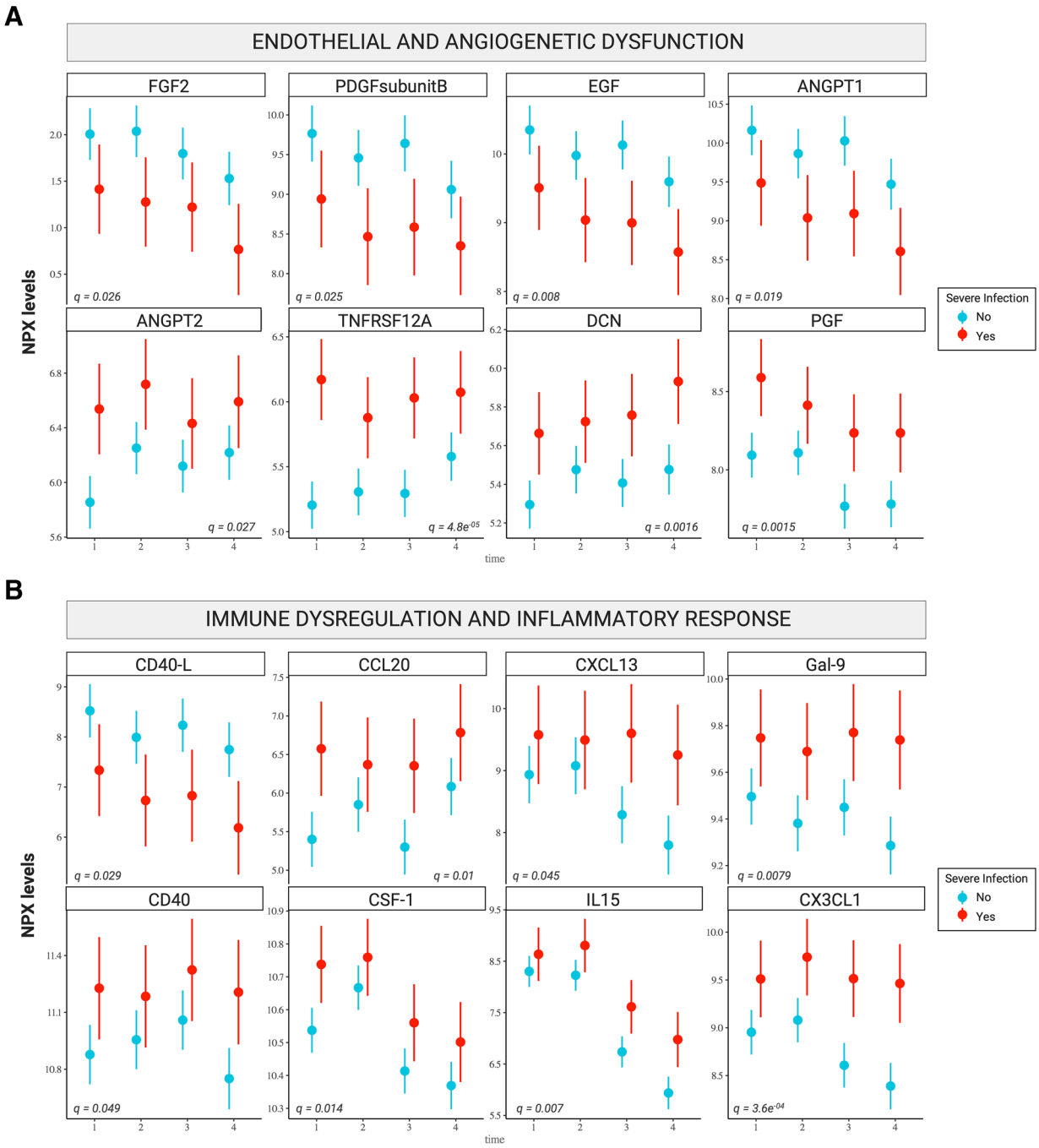

Figure 7. Patients with severe infections display progressive endothelial dysfunction and immune dysregulation. Point range plots showing the LMM estimates of mean NPX level (y-axis) per timepoint (x-axis) for the 16 candidate proteins related to either endothelial and angiogenetic dysfunction (A), or immune dysregulation and inflammatory response (B). The infection group is shown in red, while the CRS^{only} group is shown in teal. The *P* value corrected for multiple testing (*q* value) is superimposed on each panel for all Olink candidate proteins. LMM = linear mixed model; NPX = Normalized Protein eXpression.

the discrimination for severe infections compared with CRS^{only} events. In a confirmatory cohort of 125 patients, the resulting HT10 score identified patients at high risk for severe infectious complications at time of first fever. By studying longitudinal proteomic patterns, we identified endothelial dysfunction and progressive immune dysregulation in the severe infection group.

The incidence, temporal distribution, and clinical severity of infections and CRS was comparable to prior published reports.[14,21,23,25] In contrast to previous studies, we did not find an association between CRS severity and infection occurrence (Suppl. Figure S2).[14,21] Still, we did observe higher rates of grade ≥3 ICANS in the infection cohort (33% versus 7%, $P = 0.02$, Suppl. Table S2), which likely contributed to the more frequent use of high-dose glucocorticoids in these patients—an important risk factor for infectious complications.[23] The majority of both CRS and infection events occurred in the setting of neutropenia, underlining the ubiquitous nature of febrile neutropenia during the early post–CAR-T phase. In terms of routine inflammatory marker profiles, we did not observe the "double peak of IL-6 pattern" described by Luo and colleagues.[39] The authors further delineated a model

incorporating 3 cytokines (IL-8, IL1β, and interferon [IFN] γ) that predicted life-threatening infections with high sensitivity. In a pediatric cohort, Diorio et al[40] established that a normal to mildly elevated IFNγ in combination with an elevated IL1β was associated with sepsis as opposed to CRS. Although IL1β was not part of our Olink panel, we could not confirm alterations of IL-8 (q = 0.30), or IFNγ (q = 0.93) in the patients developing severe infections in our LMM. However, we would note important cohort-level differences that likely result in significant heterogeneity of the studied patient populations. These relate to the endpoint (ie, life-threatening infection, sepsis), patient population (ie, adult versus pediatric), timing of sample collection (event-triggered versus fixed time points), institutional choice of antimicrobial prophylaxis, as well as the respective CAR target antigen (ie, BCMA, CD22). Moreover, almost all patients received IL-6-receptor blockade in our study, reflecting evolving management paradigms.

Interestingly, the exploratory serum proteomic analysis revealed that the disruption of endothelial markers was already present prior to CAR-T infusion, which was especially prominent for the increase of the ratio of Angiopoietin-2 to Angiopoietin-1 (Ang-2/1 ratio). Increased Ang-2/1 ratios have been extensively studied in diverse disease contexts including as a predictor of morbidity and mortality in sepsis, critical illness, hemolytic uremic syndrome, and COVID-19.[46–51] Ang-2 is stored and rapidly released upon stimulation from endothelial cell Weibel-Palade bodies, while Ang-1 promotes endothelial stability.[52,53] In the context of CD19 CAR-T, increased Ang-2/1 ratios have been linked to enhanced blood-brain-barrier permeability in patients developing severe neurotoxicity,[54] and represent a predictor of severe CRS.[38] Notably, platelets can stabilize Ang-1,[48] which may provide an explanation as to why patients with severe baseline thrombocytopenia display a particularly high risk for infectious complications.[23] Overall, these data support a model wherein CAR-T patients are potentially predisposed for infections due to heightened endothelial permeability, downregulation of endothelial-associated antioxidant defenses, and glycocalyx shedding.[55] This in turn may also result in malformation of neutrophil extracellular traps, an important mechanism of host defense against infection.[56–59] Consistent with a response to microbial exposure, we found that serum levels of the innate immune regulators *CX3CL1, CCL20,* and *CXCL13* were increased in the severe infection group.[60,61] This was particularly evident on day 14 (Figure 6A), by which timepoint the majority of infection events had occurred. Furthermore, we found a significant alteration of the CD40/CD40-L axis, which plays a vital role in host defense against pathogens mainly via the regulation of the $CD8^+$ cytotoxic T-cell (CTL)–directed immune response.[62] For example, the activation of CD40-expressing $CD8^+$ CTLs can be facilitated either directly by CD40-L-expressing $CD4^+$ T-cells or indirectly via dendritic cells.[63,64]

Although the identified soluble serum cytokines are promising, they currently are still experimental in nature, and need to be validated externally and prospectively, across multiple clinical settings. On the other hand, PCT represents an established sepsis marker and is already available at most academic centers.[65–68] PCT is a 116-aminoacid peptide liberated into the circulation mainly in response to a stimulus of bacterial infection, and carries the advantages of a wide biological range, short time of induction after bacterial stimulus, and long half-life.[69] The identified discriminatory threshold of 1.5 µg/L is in line with the large meta-analysis of Wacker and colleagues[67] outlining the utility of PCT to distinguish sepsis from other inflammatory conditions, and is in accordance with consensus recommendations for antibiotic initiation.[66] Notably, integrating the patient-individual baseline risk of infection enhanced the utility of PCT as a biomarker to identify early infections in the setting of CRS. High CAR-HEMATOTOX scores confer an increased risk of prolonged severe neutropenia across disease entities (eg, LBCL, mantle cell lymphoma, multiple myeloma), and also reflect a pro-inflammatory state of the host, which in turn can exacerbate the risk of infectious complications.[13,23,28,70,71–73] The high sensitivity of 86% for the HT10 score in our confirmation cohort indicates an attractive negative predictive value, with the patients presenting with a low baseline risk profile and continuously low serum PCT levels unlikely to develop a severe infection. Indeed, only 3% of $HT10^{low}$ patients developed a severe nonviral infection during the study period, and none were observed until day+19 (Figure 5E). Concomitantly, this low-risk group may be spared unnecessary antibiotic exposure during the vulnerable time period of peak CAR T-cell expansion (typically weeks 1–2).[74,75]

This study has several relevant limitations. It was retrospective, uncontrolled, and limited to a moderately sized number of patients, which restrict drawing firm conclusions. Even though the infection rate was very low in the $HT10^{low}$ group, it is unclear if that would extend to patients that do no receive early anti-infective therapy in case of CRS, as is currently the standard-of-care.[23] As a result, the HT10 score needs to be validated in a prospective manner, ideally at time of first fever, before it is implemented in routine clinical use. Furthermore, the assays used to determine PCT and other inflammatory markers may differ from site to site, which may impact the determined marker thresholds. The use of high-dose glucocorticoids may have impacted cytokine marker measurements and the proteomic analysis. Viral infections were not identified in the early post-CAR-T phase, and it is unlikely that the diagnostic utility of PCT extends to viral infections,[76] though COVID-19 may represent an important exception.[77–79] Most centers currently do not perform serial PCT measurements, making it hard to extrapolate our findings to larger patient numbers. Still, these findings offer a rationale for longitudinal assessment of PCT, especially during the critical phases of CAR-T–related immunotoxicity (eg, day 1–10). If validated, we see several salient clinical applications. First, the score may guide the initiation of IV broad-spectrum antibiotic treatment and avoid unnecessary antibiotic use in patients with a very low risk of severe infections (ie, low HT10 score, stable hemodynamics and respiratory status).[65,66] Reducing antibiotic exposure appears especially pertinent given recent evidence pointing towards the immunomodulatory role of the gut microbiome during CAR-T therapy.[33–35] Second, the score may be incorporated into decision making algorithms regarding in- versus outpatient management of CAR-T patients at time of first fever.[36,80] Finally, future preventive strategies may target the endothelial compartment or dysregulated immune response at an early time point as a means to prevent severe infectious complications in CAR T-cell patients.

In conclusion, severe infections and CRS present with distinct inflammatory signatures following CD19 CAR-T. By incorporating dynamic changes in serum inflammatory markers into baseline prognostication models, early infections could be identified in the setting of coincident CRS, enabling more patient-specific toxicity management.

ACKNOWLEDGMENTS

First and foremost, the authors thank the patients and their families for their participation in this study. We would like to thank Simon Forsberg from Olink Proteomics for the help with the bioinformatic analysis.

AUTHOR CONTRIBUTIONS

Conceptualization: KR, VLB; investigation: KR, GI, VB, LLC, SK, RH, AP, NM, FH, LF, PK, CS, DMCdS, JLP, FM, AAM, MS, MvB-B, PB, MS, VLB; formal analysis and visualization: KR, VLB; methodology: KR, VLB; writing original draft: KR, VLB; writing review and editing: KR, GI, VB, MvB-B, AM, WB, PB, MS, VLB. All authors read and approved the final manuscript.

DATA AVAILABILITY

For original data and material, please contact kai.rejeski@med.uni-muenchen.de.

DISCLOSURES

KR: Kite/Gilead - Research Funding and travel support; Novartis - Honoraria. VB: Novartis - Honoraria, Research Funding; Gilead - Consultancy, Research Funding; Celgene - Research Funding; Janssen - Honoraria, Research Funding; Roche - Research funding; Takeda - Research funding. GI: Consultancy and Honoraria - Novartis, Roche, Kite/Gilead, Bristol-Myers Squibb, Abbvie, Janssen, Sandoz, Miltenyi, AstraZeneca. MD: Research Support - Abbvie, Bayer, BMS/Celgene, Kite/Gilead, Janssen, Roche; Honoraria - Amgen, Astra Zeneca, Kite/Gilead, Janssen, Lilly, Novartis, Roche; Consultancy - Astra Zeneca, Beigene, BMS/Celgene, Kite/Gilead, Janssen, Novartis, Roche; Journal Editor - HemaSphere. MvB-B: Consultancy, Research Funding and Honoraria - MSD Sharp & Dohme, Novartis, Roche, Kite/Gilead, Bristol-Myers Squibb, Astellas, Mologen, and Miltenyi. PB declares having received honoraria from Allogene, Amgen, BMS/CELGENE, Jansen, Kite/Gilead, Incyte, Jazz Pharmaceuticals, Miltenyi Biomedicine, Novartis and Nektar. MS: Morphosys - Research Funding; Novartis - Consultancy, Research Funding; Janssen - Consultancy; Seattle Genetics - Research Funding; AMGEN - Consultancy, Honoraria, Research Funding; Celgene - Consultancy, Honoraria; Kite/Gilead - Consultancy, Honoraria, Research Funding; Roche AG - Consultancy, Research Funding. VLB: AMGEN - Honoraria; Celgene - Research Funding; Pfizer - Honoraria; Kite/Gilead - Research Funding, Honoraria; Novaritis - Honoraria, Consultancy/Advisory; BMS - Consultancy/Advisory; Takeda - Consultancy/Advisory. None of the mentioned conflicts of interest were related to financing of the content of this manuscript. All the other authors have no conflicts of interest to disclose.

SOURCES OF FUNDING

This work was supported by a grant within the Gilead Research Scholar Program (to KR, MS). Deutsche Forschungsgemeinschaft (DFG, German Research Foundation) research grant provided within the Sonderforschungbereich SFB-TRR 388/1 2021 – 452881907, and DFG research grant 451580403 (to MS). The work was further supported by the Bavarian Elite Graduate Training Network (to MS), the Wilhelm-Sander Stiftung (to MS, project no. 2018.087.1), the Else-Kröner-Fresenius Stiftung (to MS), and the Bavarian Center for Cancer Research (BZKF). KR received a fellowship from the School of Oncology of the German Cancer Consortium (DKTK). KR, VB, and VLB were funded by the Else Kröner Forschungskolleg (EKFK) within the Munich Clinician Scientist Program (MCSP).

REFERENCES

1. Locke FL, Ghobadi A, Jacobson CA, et al. Long-term safety and activity of axicabtagene ciloleucel in refractory large B-cell lymphoma (ZUMA-1): a single-arm, multicentre, phase 1-2 trial. *Lancet Oncol*. 2019;20:31–42.
2. Schuster SJ, Bishop MR, Tam CS, et al. Tisagenlecleucel in adult relapsed or refractory diffuse large B-Cell lymphoma. *N Engl J Med*. 2019;380:45–56.
3. Wang M, Munoz J, Goy A, et al. KTE-X19 CAR T-cell therapy in relapsed or refractory mantle-cell lymphoma. *N Engl J Med*. 2020;382:1331–1342.
4. Crump M, Neelapu SS, Farooq U, et al. Outcomes in refractory diffuse large B-cell lymphoma: results from the international SCHOLAR-1 study. *Blood*. 2017;130:1800–1808.
5. Bethge WA, Martus P, Schmitt M, et al. GLA/DRST real-world outcome analysis of CAR-T cell therapies for large B-cell lymphoma in Germany. *Blood*. 2022;140:349–358.
6. Nastoupil LJ, Jain MD, Feng L, et al. Standard-of-care axicabtagene ciloleucel for relapsed or refractory large B-cell lymphoma: results from the US lymphoma CAR T consortium. *J Clin Oncol*. 2020;38:3119–3128.
7. Jacobson CA, Locke FL, Ma L, et al. Real-world evidence of axicabtagene ciloleucel for the treatment of large B cell lymphoma in the United States. *Transplant Cell Ther*. 2022;28:581.e1–581.e8.
8. Karschnia P, Rejeski K, Winkelmann M, et al. Toxicities and response rates of secondary CNS lymphoma after adoptive immunotherapy with CD19-directed chimeric antigen receptor T cells. *Neurology*. 2022;98:884–889.
9. Morris EC, Neelapu SS, Giavridis T, et al. Cytokine release syndrome and associated neurotoxicity in cancer immunotherapy. *Nat Rev Immunol*. 2021;22:85–96.
10. Lee DW, Santomasso BD, Locke FL, et al. ASTCT consensus grading for cytokine release syndrome and neurologic toxicity associated with immune effector cells. *Biol Blood Marrow Transplant*. 2019;25:625–638.
11. Dos Santos DMC, Rejeski K, Winkelmann M, et al. Increased visceral fat distribution and body composition impact cytokine release syndrome onset and severity after CD19 CAR-T in advanced B-cell malignancies. *Haematologica*. 2022;107:2096–2107.
12. Rejeski K, Kunz WG, Rudelius M, et al. Severe Candida glabrata pancolitis and fatal Aspergillus fumigatus pulmonary infection in the setting of bone marrow aplasia after CD19-directed CAR T-cell therapy - a case report. *BMC Infect Dis*. 2021;21:121.
13. Rejeski K, Perez Perez A, Sesques P, et al. CAR-HEMATOTOX: a model for CAR T-cell related hematological toxicity in relapsed/refractory large B-cell lymphoma. *Blood*. 2021;138:2499–2513.
14. Logue JM, Zucchetti E, Bachmeier CA, et al. Immune reconstitution and associated infections following axicabtagene ciloleucel in relapsed or refractory large B-cell lymphoma. *Haematologica*. 2020;106:978–986.
15. Jain T, Knezevic A, Pennisi M, et al. Hematopoietic recovery in patients receiving chimeric antigen receptor T-cell therapy for hematologic malignancies. *Blood Adv*. 2020;4:3776–3787.
16. Rejeski K, Wu Z, Blumenberg V, et al. Oligoclonal T-cell expansion in a patient with bone marrow failure after CD19 CAR-T for richter transformed DLBCL. *Blood*. 2022;140:2175–2179.
17. Rejeski K, Burchert A, Iacoboni G, et al. Safety and feasibility of stem cell boost as a salvage therapy for severe hematotoxicity after CD19 CAR T-cell therapy. *Blood Adv*. 2022;6:4719–4725.
18. Fried S, Avigdor A, Bielorai B, et al. Early and late hematologic toxicity following CD19 CAR-T cells. *Bone Marrow Transplant*. 2019;54:1643–1650.
19. Park JH, Riviere I, Gonen M, et al. Long-term follow-up of CD19 CAR therapy in acute lymphoblastic leukemia. *N Engl J Med*. 2018;378:449–459.
20. Hill JA, Seo SK. How I prevent infections in patients receiving CD19-targeted chimeric antigen receptor T cells for B-cell malignancies. *Blood*. 2020;136:925–935.
21. Hill JA, Li D, Hay KA, et al. Infectious complications of CD19-targeted chimeric antigen receptor-modified T-cell immunotherapy. *Blood*. 2018;131:121–130.
22. Wudhikarn K, Pennisi M, Garcia-Recio M, et al. DLBCL patients treated with CD19 CAR T cells experience a high burden of organ toxicities but low nonrelapse mortality. *Blood Adv*. 2020;4:3024–3033.
23. Rejeski K, Perez A, Iacoboni G, et al. The CAR-HEMATOTOX risk-stratifies patients for severe infections and disease progression after CD19 CAR-T in R/R LBCL. *J ImmunoTher Cancer*. 2022;10:e004475.
24. Gudiol C, Lewis RE, Strati P, et al. Chimeric antigen receptor T-cell therapy for the treatment of lymphoid malignancies: is there an excess risk for infection? *Lancet Haematol*. 2021;8:e216–e228.
25. Wudhikarn K, Palomba ML, Pennisi M, et al. Infection during the first year in patients treated with CD19 CAR T cells for diffuse large B cell lymphoma. *Blood Cancer J*. 2020;10:79.
26. Fajgenbaum DC, June CH. Cytokine Storm. *N Engl J Med*. 2020;383:2255–2273.
27. Juluri KR, Wu V, Voutsinas JM, et al. Severe cytokine release syndrome is associated with hematologic toxicity following CD19 CAR T-cell therapy. *Blood Adv*. 2021;6:2055–2068.
28. Taplitz RA, Kennedy EB, Bow EJ, et al. Antimicrobial prophylaxis for adult patients with cancer-related immunosuppression: ASCO and IDSA clinical practice guideline update. *J Clin Oncol*. 2018;36:3043–3054.
29. Spellberg B, Doi Y. The rise of fluoroquinolone-resistant escherichia coli in the community: scarier than we thought. *J Infect Dis*. 2015;212:1853–1855.
30. Lautenbach E, Metlay JP, Bilker WB, et al. Association between fluoroquinolone resistance and mortality in Escherichia coli and Klebsiella pneumoniae infections: the role of inadequate empirical antimicrobial therapy. *Clin Infect Dis*. 2005;41:923–929.
31. Trecarichi EM, Tumbarello M, Spanu T, et al. Incidence and clinical impact of extended-spectrum-beta-lactamase (ESBL) production and fluoroquinolone resistance in bloodstream infections caused by Escherichia coli in patients with hematological malignancies. *J Infect*. 2009;58:299–307.
32. Bow EJ. Fluoroquinolones, antimicrobial resistance and neutropenic cancer patients. *Curr Opin Infect Dis*. 2011;24:545–553.
33. Schubert ML, Rohrbach R, Schmitt M, et al. The potential role of the intestinal micromilieu and individual microbes in the immunobiology of chimeric antigen receptor T-cell therapy. *Front Immunol*. 2021;12:670286.
34. Smith M, Dai A, Ghilardi G, et al. Gut microbiome correlates of response and toxicity following anti-CD19 CAR T cell therapy. *Nat Med*. 2022;28:713–723.

35. Blumenberg V, Busch G, Baumann S, et al. High bacterial abundances of dorea and pediococcus in the gut microbiome linked to expansion, immune checkpoint expression and efficacy of CD19-directed CAR T-cells in patients with r/r DLBCL. *Blood*. 2021;138(Suppl 1):2792–2792.
36. Myers GD, Verneris MR, Goy A, et al. Perspectives on outpatient administration of CAR-T cell therapy in aggressive B-cell lymphoma and acute lymphoblastic leukemia. *J ImmunoTher Cancer*. 2021;9:e002056.
37. Teachey DT, Lacey SF, Shaw PA, et al. Identification of predictive biomarkers for cytokine release syndrome after chimeric antigen receptor T-cell therapy for acute lymphoblastic leukemia. *Cancer Discov*. 2016;6:664–679.
38. Hay KA, Hanafi LA, Li D, et al. Kinetics and biomarkers of severe cytokine release syndrome after CD19 chimeric antigen receptor-modified T-cell therapy. *Blood*. 2017;130:2295–2306.
39. Luo H, Wang N, Huang L, et al. Inflammatory signatures for quick diagnosis of life-threatening infection during the CAR T-cell therapy. *J ImmunoTher Cancer*. 2019;7:271.
40. Diorio C, Shaw PA, Pequignot E, et al. Diagnostic biomarkers to differentiate sepsis from cytokine release syndrome in critically ill children. *Blood Adv*. 2020;4:5174–5183.
41. Shimabukuro-Vornhagen A, Godel P, Subklewe M, et al. Cytokine release syndrome. *J ImmunoTher Cancer*. 2018;6:56.
42. Young JH, Logan BR, Wu J, et al. Infections after transplantation of bone marrow or peripheral blood stem cells from unrelated donors. *Biol Blood Marrow Transplant*. 2016;22:359–370.
43. Greenbaum U, Strati P, Saliba RM, et al. CRP and ferritin in addition to the EASIX score predict CAR-T-related toxicity. *Blood Adv*. 2021;5:2799–2806.
44. Filbin MR, Mehta A, Schneider AM, et al. Longitudinal proteomic analysis of severe COVID-19 reveals survival-associated signatures, tissue-specific cell death, and cell-cell interactions. *Cell Rep Med*. 2021;2:100287.
45. Nahi H, Chrobok M, Meinke S, et al. Autologous NK cells as consolidation therapy following stem cell transplantation in multiple myeloma. *Cell Rep Med*. 2022;3:100508.
46. Page AV, Tarr PI, Watkins SL, et al. Dysregulation of angiopoietin 1 and 2 in Escherichia coli O157:H7 infection and the hemolytic-uremic syndrome. *J Infect Dis*. 2013;208:929–933.
47. Mikacenic C, Hahn WO, Price BL, et al. Biomarkers of endothelial activation are associated with poor outcome in critical illness. *PLoS One*. 2015;10:e0141251.
48. Page AV, Liles WC. Biomarkers of endothelial activation/dysfunction in infectious diseases. *Virulence*. 2013;4:507–516.
49. Ricciuto DR, dos Santos CC, Hawkes M, et al. Angiopoietin-1 and angiopoietin-2 as clinically informative prognostic biomarkers of morbidity and mortality in severe sepsis. *Crit Care Med*. 2011;39:702–710.
50. Smadja DM, Guerin CL, Chocron R, et al. Angiopoietin-2 as a marker of endothelial activation is a good predictor factor for intensive care unit admission of COVID-19 patients. *Angiogenesis*. 2020;23:611–620.
51. Villa E, Critelli R, Lasagni S, et al. Dynamic angiopoietin-2 assessment predicts survival and chronic course in hospitalized patients with COVID-19. *Blood Adv*. 2021;5:662–673.
52. Fiedler U, Scharpfenecker M, Koidl S, et al. The Tie-2 ligand angiopoietin-2 is stored in and rapidly released upon stimulation from endothelial cell Weibel-Palade bodies. *Blood*. 2004;103:4150–4156.
53. Brindle NP, Saharinen P, Alitalo K. Signaling and functions of angiopoietin-1 in vascular protection. *Circ Res*. 2006;98:1014–1023.
54. Gust J, Hay KA, Hanafi LA, et al. Endothelial activation and blood-brain barrier disruption in neurotoxicity after adoptive immunotherapy with CD19 CAR-T cells. *Cancer Discov*. 2017;7:1404–1419.
55. Ince C, Mayeux PR, Nguyen T, et al. The endothelium in sepsis. *Shock*. 2016;45:259–270.
56. Camicia G, Pozner R, de Larranaga G. Neutrophil extracellular traps in sepsis. *Shock*. 2014;42:286–294.
57. Fuchs TA, Abed U, Goosmann C, et al. Novel cell death program leads to neutrophil extracellular traps. *J Cell Biol*. 2007;176:231–241.
58. Bianchi M, Hakkim A, Brinkmann V, et al. Restoration of NET formation by gene therapy in CGD controls aspergillosis. *Blood*. 2009;114:2619–2622.
59. Bianchi M, Niemiec MJ, Siler U, et al. Restoration of anti-Aspergillus defense by neutrophil extracellular traps in human chronic granulomatous disease after gene therapy is calprotectin-dependent. *J Allergy Clin Immunol*. 2011;127:1243–52.e7.
60. Gasteiger G, D'Osualdo A, Schubert DA, et al. Cellular innate immunity: an old game with new players. *J Innate Immun*. 2017;9:111–125.
61. Vilgelm AE, Richmond A. Chemokines modulate immune surveillance in tumorigenesis, metastasis, and response to immunotherapy. *Front Immunol*. 2019;10:333.
62. Elgueta R, Benson MJ, de Vries VC, et al. Molecular mechanism and function of CD40/CD40L engagement in the immune system. *Immunol Rev*. 2009;229:152–172.
63. Ahmed KA, Wang L, Munegowda MA, et al. Direct in vivo evidence of CD4+ T cell requirement for CTL response and memory via pMHC-I targeting and CD40L signaling. *J Leukoc Biol*. 2012;92:289–300.
64. Bourgeois C, Rocha B, Tanchot C. A role for CD40 expression on CD8+ T cells in the generation of CD8+ T cell memory. *Science*. 2002;297:2060–2063.
65. Schuetz P, Briel M, Christ-Crain M, et al. Procalcitonin to guide initiation and duration of antibiotic treatment in acute respiratory infections: an individual patient data meta-analysis. *Clin Infect Dis*. 2012;55:651–662.
66. Schuetz P, Wirz Y, Sager R, et al. Procalcitonin to initiate or discontinue antibiotics in acute respiratory tract infections. *Cochrane Database Syst Rev*. 2017;10:CD007498.
67. Wacker C, Prkno A, Brunkhorst FM, et al. Procalcitonin as a diagnostic marker for sepsis: a systematic review and meta-analysis. *Lancet Infect Dis*. 2013;13:426–435.
68. Assicot M, Gendrel D, Carsin H, et al. High serum procalcitonin concentrations in patients with sepsis and infection. *Lancet*. 1993;341:515–518.
69. Dandona P, Nix D, Wilson MF, et al. Procalcitonin increase after endotoxin injection in normal subjects. *J Clin Endocrinol Metab*. 1994;79:1605–1608.
70. Locke FL, Rossi JM, Neelapu SS, et al. Tumor burden, inflammation, and product attributes determine outcomes of axicabtagene ciloleucel in large B-cell lymphoma. *Blood Adv*. 2020;4:4898–4911.
71. Jain MD, Zhao H, Wang X, et al. Tumor interferon signaling and suppressive myeloid cells are associated with CAR T-cell failure in large B-cell lymphoma. *Blood*. 2021;137:2621–2633.
72. Rejeski K, Hansen DK, Bansal R, et al. The CAR-Hematotox Score As a Prognostic Model of Toxicity and Response in Patients Receiving BCMA-Directed CAR-T for Relapsed/Refractory Multiple Myeloma. *Blood*. 2022;140(Suppl 1):7506–7508.
73. Rejeski K, Wang Y, Albanyan O, et al. The CAR-Hematotox Score Identifies Patients at High Risk for Hematological Toxicity, Infections and Poor Clinical Outcomes Following Brexucabtagene Autoleucel in Relapsed/Refractory Mantle Cell Lymphoma. *Blood*. 2022;140(Suppl 1):651–653.
74. Peinelt A, Bremm M, Kreyenberg H, et al. Monitoring of circulating CAR T cells: validation of a flow cytometric assay, cellular kinetics, and phenotype analysis following tisagenlecleucel. *Front Immunol*. 2022;13:830773.
75. Ayuk FA, Berger C, Badbaran A, et al. Axicabtagene ciloleucel in vivo expansion and treatment outcome in aggressive B-cell lymphoma in a real-world setting. *Blood Adv*. 2021;5:2523–2527.
76. Kamat IS, Ramachandran V, Eswaran H, et al. Procalcitonin to distinguish viral from bacterial pneumonia: a systematic review and meta-analysis. *Clin Infect Dis*. 2020;70:538–542.
77. Hu R, Han C, Pei S, et al. Procalcitonin levels in COVID-19 patients. *Int J Antimicrob Agents*. 2020;56:106051.
78. Tong-Minh K, van der Does Y, Engelen S, et al. High procalcitonin levels associated with increased intensive care unit admission and mortality in patients with a COVID-19 infection in the emergency department. *BMC Infect Dis*. 2022;22:165.
79. Kaal A, Snel L, Dane M, et al. Diagnostic yield of bacteriological tests and predictors of severe outcome in adult patients with COVID-19 presenting to the emergency department. *Emerg Med J*. 2021;38:685–691.
80. Borogovac A, Keruakous A, Bycko M, et al. Safety and feasibility of outpatient chimeric antigen receptor (CAR) T-cell therapy: experience from a tertiary care center. *Bone Marrow Transplant*. 2022;57:1025–1027.